

# Modal analysis of wave propagation in dispersive media

M. Ismail Abdelrahman\* and B. Gralak

Aix Marseille Univ, CNRS, Centrale Marseille, Institut Fresnel, Marseille, France

Surveys on wave propagation in dispersive media have been limited since the pioneering work of Sommerfeld [Ann. Phys. **349**, 177 (1914)] by the presence of branches in the integral expression of the wave function. In this article, a method is proposed to eliminate these critical branches and hence to establish a modal expansion of the time-dependent wave function. The different components of the transient waves are physically interpreted as the contributions of distinct sets of modes and characterized accordingly. Then, the modal expansion is used to derive a modified analytical expression of the Sommerfeld precursor improving significantly the description of the amplitude and the oscillating period up to the arrival of the Brillouin precursor. The proposed method and results apply to all waves governed by the Helmholtz equations.

## I. INTRODUCTION

The modern developments of wave propagation in linear homogeneous dispersive media have been initiated by Sommerfeld [1] and Brillouin [2]. The main motivation was to investigate the causality principle [3], when strong dispersion holds, and the notion of signal velocity [2]. These pioneering works led to the description of the Sommerfeld and Brillouin precursors (also known as forerunners), which are transient waves preceding the main propagating signal. Analyzing these precursors is unavoidable for a wideband signal propagating in dispersive media since, for instance, they are responsible for the pulse distortion in communication systems [4, 5]. Moreover, they can be useful for probing biological samples [6], for underwater communications [7], and for warning systems based on the early detection of precursors [8]. They have been observed at the microwave and optical frequencies [7, 9–12]. Similar behavior occurs in other situations such as spatially-dispersive media [13], photonic crystals [14], acoustic waves [15, 16], gravity waves [8], or more generally, all waves described by Helmholtz equations. More recently, the introduction of negative index materials [17–20], metamaterials and transformation optics [21–23] caused an additional interest for the dispersion phenomenon [17]. Hence, the effect of dispersion has been recently investigated in the cases of the flat lens [24–28] and invisibility systems [29].

Since 1914 and the work of Sommerfeld [1], the analysis of wave propagation in dispersive media has been restricted by the presence of branch-cuts in the solution to the wave equation for the electric field  $E$  [30]. Let a sinusoidal source of frequency  $\omega_s$  be switched on at an initial time  $t = 0$  in an infinite dispersive medium of relative permittivity  $\varepsilon(\omega)$ . Then, the temporal behavior of the field at a distance  $x$  from the source is given by the following integral in the complex frequency domain [2]:

$$E_\infty(x, t) = -\frac{E_0}{2\pi} \int_{\Gamma} d\omega e^{-i\omega t} \frac{\omega_s}{\omega^2 - \omega_s^2} e^{i\omega \sqrt{\varepsilon(\omega)} x/c}, \quad (1)$$

where  $E_0$  is proportional to the source amplitude at  $x = 0$ ,  $c$  is the light velocity in vacuum,  $\sqrt{\varepsilon(\omega)}$  is the refractive index of the medium, and the integration path  $\Gamma$  is a line parallel to the real axis in the half plane of complex frequencies with positive imaginary part. The main difficulty to compute the integral (1) is the presence of the square root  $\sqrt{\varepsilon(\omega)}$ , which induces branch-points and branch-cuts constituting a severe drawback for a direct evaluation. This issue has been mainly addressed using numerical methods [31] and asymptotic approaches [2, 32–35], the latter requiring a specific form of the dispersion relation [36, 37]. As for the group velocity approximation, it usually fails to analyze wideband pulses [30]. The book of Oughstun [38] can be consulted for an extensive bibliography.

In this article, a novel approach is proposed to remove this critical branch-cut: instead of wave propagation in an infinite homogeneous medium, wave transmission through a slab of a thickness  $d$  is considered (see Fig. 1). In this case, it is shown that no branches exist in the integral expression and, consequently, the transmitted field can be evaluated in the time domain using a discrete modal expansion. This modal expansion is then used to interpret and characterize all the components of the transient waves, e.g. the Sommerfeld and Brillouin precursors. Interestingly, the transient waves at the onset of the transmitted field with velocities close to  $c$ , which experience a near unity permittivity, are matching their counterparts in infinite media since the slab reflections are negligible. This striking resemblance allows the use of the proposed modal expansion to derive a mod-

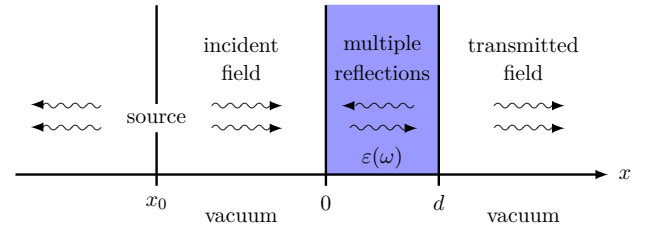


FIG. 1. A slab of a homogeneous medium of arbitrarily dispersion is illuminated in normal incidence (1-D problem).

\* m.abdelrahman@fresnel.fr

ified analytical expression of the Sommerfeld precursor which, compared to the original expression [1], improves significantly the amplitude and periodicity description.

## II. MODAL EXPANSION

The considered system is made of a dispersive slab with permittivity  $\varepsilon(\omega)$  and thickness  $d$ , as represented in Fig. 1. Normalized (dimensionless) quantities are used to describe the problem in a simple way,

$$\omega (d/c) \longrightarrow \omega, \quad (t - |x_0|/c) (c/d) \longrightarrow t. \quad (2)$$

Assuming the surrounding medium to be vacuum, the system can be treated as a symmetric passive Fabry-Pérot resonator with the multiple reflections effect. The reflection coefficient  $\rho$  of the slab interface is

$$\rho(\omega) = \frac{1 - \sqrt{\varepsilon(\omega)}}{1 + \sqrt{\varepsilon(\omega)}}, \quad (3)$$

and the transmitted field can be analyzed using the resonator transmission function  $T(\omega)$  [39]:

$$T(\omega) = \frac{[1 - \rho^2(\omega)] e^{i\omega\sqrt{\varepsilon(\omega)}}}{1 - \rho^2(\omega) e^{2i\omega\sqrt{\varepsilon(\omega)}}}. \quad (4)$$

It is stressed that, after some algebra, this transmission function can be expressed as

$$\frac{1}{T(\omega)} = \cos[\omega\sqrt{\varepsilon(\omega)}] - i \frac{1 + \varepsilon(\omega)}{2} \frac{\sin[\omega\sqrt{\varepsilon(\omega)}]}{\sqrt{\varepsilon(\omega)}}, \quad (5)$$

excluding the case  $T = 0$ , which is in practice irrelevant to the study herein. Indeed, this expression shows that

$T(\omega)$  is an even function of  $\sqrt{\varepsilon(\omega)}$ ; this important remark implies the absence of branches of square roots of the permittivity in  $T(\omega)$ . Similar to Eq. (1), the time dependence of the transmitted field at the output is

$$E_T(t) = -\frac{E_0}{2\pi} \int_{\Gamma} d\omega e^{-i\omega t} \frac{\omega_s}{\omega^2 - \omega_s^2} T(\omega), \quad (6)$$

where  $E_0(\omega)$  is the incident field at  $x = 0$ . This integration contains neither branch-points nor branch-cuts, which is the key argument of this study. Accordingly, it is possible to derive a closed-form expression of the transmitted field in terms of the contributions of the poles of the integrand, corresponding to a modal expansion.

The transmitted field is then resolved into two main contributions:  $E_s(t)$  the contribution of the source poles  $\pm\omega_s$ , and  $E_r(t)$  the contribution of the resonator poles  $\{\omega_q, q \text{ integer}\}$  of  $T(\omega)$ . Namely,

$$E_T(t) = \theta(t - t_0) E_s(t) + \theta(t - t_0) E_r(t), \quad (7)$$

where  $\theta$  is Heaviside unit step function;  $\theta(t) = 0$  for  $t < 0$  and  $\theta(t) = 1$  for  $t > 0$ . In normalized units,  $t_0 = 1$  is the time needed for the front of the wave to reach from the input to the output of the slab. That preserves causality since no signal can travel faster than light. Using the Hermitian property of the transmission function  $\overline{T(\omega)} = T(-\bar{\omega})$ , one obtains

$$E_s(t) = -\text{Im}[e^{-i\omega_s t} T(\omega_s) E_0(\omega_s)], \quad (8)$$

where “Im” means the imaginary part. The second contribution  $E_r(t)$  can be expressed as

$$E_r(t) = i \sum_{\{\omega_q\}} e^{-i\omega_q t} \frac{\omega_s}{\omega_q^2 - \omega_s^2} E_0(\omega_q) \left[ \frac{\partial T^{-1}}{\partial \omega}(\omega_q) \right]^{-1}. \quad (9)$$

The expression of the residues at  $\omega_q$  is given by

$$\frac{\partial T^{-1}}{\partial \omega}(\omega_q) = -i \frac{1 + \varepsilon_q}{2} \left[ 1 + \frac{\omega_q}{2\varepsilon_q} \frac{\partial \varepsilon}{\partial \omega}(\omega_q) \right] \cos[\omega_q \sqrt{\varepsilon_q}] - \left[ \varepsilon_q + \frac{2\omega_q \varepsilon_q + i(\varepsilon_q - 1)}{4\varepsilon_q} \frac{\partial \varepsilon}{\partial \omega}(\omega_q) \right] \frac{\sin[\omega_q \sqrt{\varepsilon_q}]}{\sqrt{\varepsilon_q}}, \quad (10)$$

where  $\varepsilon_q \equiv \varepsilon(\omega_q)$ . Each term in Eq. (9) represents the contribution of a pole  $\omega_q$  to the transmitted field.

## III. FIELD EVALUATION IN TIME DOMAIN

An elementary example is presented for a Drude-Lorentz medium with a dispersive permittivity [40]

$$\varepsilon(\omega) = 1 - \frac{\Omega^2}{\omega^2 - \omega_0^2 + i\omega\gamma}, \quad (11)$$

where  $\Omega$  is a coefficient of the medium related to the electron density,  $\omega_0$  is the resonance frequency of the dispersive medium, and  $\gamma$  is the absorption coefficient. All the aforementioned quantities are normalized, similar to (2). Numerical methods shall be used to compute the poles of  $T(\omega)$  for complex systems [41, 42], with the possibility to implement linearization techniques of the frequency dispersion [43, 44]. In the present work, Muller algorithm is used for a numerical solution based on the secant method [45]. In addition, the simple system considered here al-

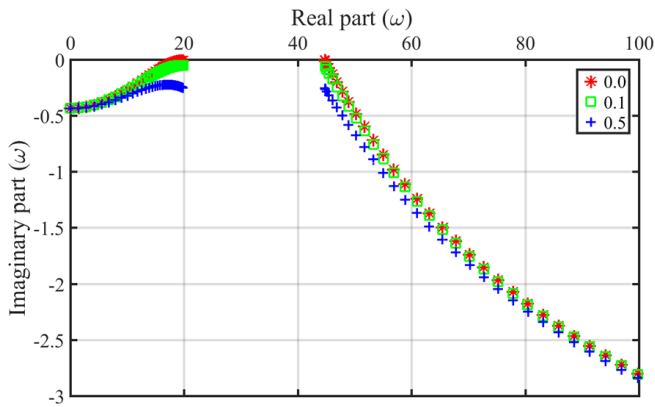


FIG. 2. The resonator poles (modes) of a Lorentz medium of  $\omega_0 = 20$  and  $\Omega = 40$  for the absorption coefficients  $\gamma = 0, 0.1$  and  $0.5$ . The set of poles is symmetric with respect to the imaginary axis.

lowers the derivation of asymptotic analytical expressions for the poles, as presented in the appendix.

Figure 2 shows the resonator poles  $\{\omega_q\}$  of a given test case of  $\omega_0 = 20$ ,  $\Omega = 40$  for different values of the absorption coefficient:  $\gamma = 0, 0.1$ , and  $0.5$ . For such a dispersive system, the imaginary part of the poles is frequency dependent: it represents the losses due to absorption and the output coupling through the interfaces. The poles in Fig. 2 can be classified into two groups. The first group is poles below resonance frequency  $\omega_0$ , which are mainly responsible for the Brillouin precursor. The second group is poles above the plasma frequency  $\omega_p = \sqrt{\omega_0^2 + \Omega^2}$ , i.e. 44.7 in the given example. These high-frequency poles constitute the wavefront of the signal with a velocity near  $c$ , i.e. the Sommerfeld precursor. No poles exist in between since the permittivity is negative in this region. The absorption clearly affects the poles near both resonance and plasma frequencies.

The poles  $\{\omega_q\}$  are then used to evaluate and interpret the transmitted field as given by Eqs. (7) to (10). Figure 3 shows the temporal evolution of the transmitted field  $E_T(t)$  of the given test in Fig. 2 for a near-resonance excitation of  $\omega_s = 15$ , where the dispersion effect on the signal propagation is significant. The amplitude of the incident field is set to be unity at the input of the slab. As depicted in Fig. 3, the signal shows successive various temporal regimes since each frequency component of the signal can be considered to have its own velocity. At the onset of the signal (highlighted region), the high frequency but low amplitude oscillations correspond to the Sommerfeld precursor, followed by the low-frequency oscillations constituting the Brillouin precursor. Afterward, the main signal starts to build up at the output, until it reaches the steady level  $|T(\omega_s)|$  after few round trips inside the resonator. The solution accuracy depends on the precision of the poles. The effect of absorption on the precursors is negligible since both Sommerfeld and Brillouin poles are far away from the resonance.

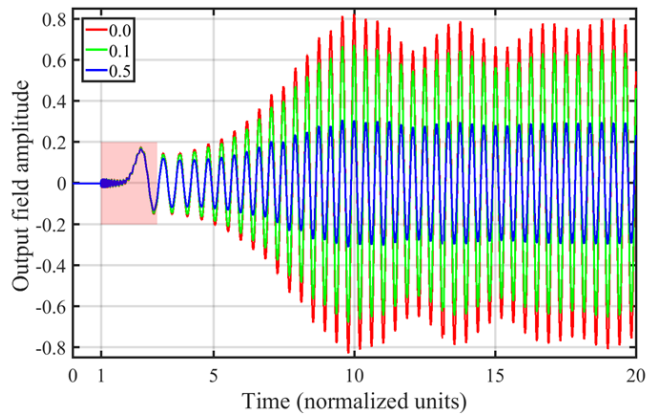


FIG. 3. The temporal response of a Lorentz resonator of  $\omega_0 = 20$ ,  $\Omega = 40$  and excited by a sinusoidal source at  $\omega_s = 15$ , switched on at  $t = 0$ , for the different absorption coefficients  $\gamma = 0, 0.1$  and  $0.5$ .

#### IV. PRECURSORS

The main advantage of the modal approach is the direct link between the poles shown in Fig. 2, and the different components of the precursors shown in Fig. 4.a): the highlighted region at Fig. 3. For instance, the curve in 4.b) illustrates the sole contribution of low-frequency poles that is shown to be responsible for the Brillouin precursor. The arrival time of this Brillouin precursor peak  $t_B$  can be directly evaluated using the group velocity approximation since, in the low-frequency regime, the dispersion is weak. As confirmed by the curve 4.b), this time  $t_B$  is approximately given by  $\sqrt{\varepsilon(\omega = 0)} \approx 2.24$ . The contribution of the poles near resonance is negligible since the associated reflectivity at the interfaces is close to unity, refer to the appendix for a detailed discussion. Figure 4.c) shows the contribution of the high-frequency poles above the plasma frequency  $\omega_p$ : it starts with the Sommerfeld precursor, corresponding to the highest frequencies, then followed by the frequencies gradually decreasing down to  $\omega_p$ , as confirmed by the temporal period  $\tau_p = 2\pi/\omega_p \approx 0.14$  for  $t \geq 2$ .

It is important to notice that this method is applicable to accurately describe the transient waves propagating in an infinite dispersive medium. Indeed, the curves derived from Eqs. (1) and (6) appear to be indiscernible at the onset of the signal, i.e. for the wave components with group velocity close to  $c$ , as clearly shown in Fig. 4.a). That motivates the derivation of the Sommerfeld precursor using the proposed method given that only the high-frequency poles above  $\omega_p$  contributes, as confirmed by Figs. 4.b) and 4.c). An estimate of the corresponding poles above  $\omega_p$  is provided in the appendix, Eq. (A.34): for integers  $q \in \mathbb{Z}$ ,

$$\omega_q \approx q\pi \left[ 1 + \frac{\Omega^2/2}{q^2\pi^2} \right] - i \ln \frac{4q^2\pi^2}{\Omega^2}. \quad (12)$$

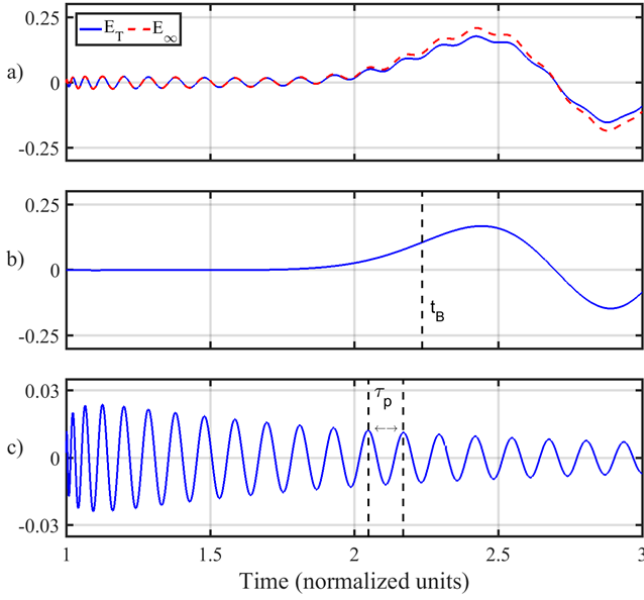


FIG. 4. a) The total transmitted signal  $E_T$  for the case of a slab [blue curve, Eq. (6)] at the highlighted region in Fig. 3 showing the Sommerfeld precursor starting at  $t = 1$  followed by the Brillouin precursor, compared to the infinite medium solution  $E_\infty$  [red dashed, Eq. (1)]. b) and c) The contributions of the low and high-frequency groups of poles.

The corresponding residues are determined using Eq. (10) which, in this situation of high frequencies, gives  $i \exp[i\omega_q \sqrt{\varepsilon_q}]/(2\sqrt{\varepsilon_q})$  at the same order of approximation. Assuming  $\omega_q \gg \omega_s$  and  $\omega_q \gg \omega_0$ , Eq. (9) can be used to obtain an estimate of  $E_p(t)$ , the contribution of the high-frequency poles:

$$E_p(t) \approx -\omega_s \sum_q \frac{\exp[-i\omega_q t]}{\omega_q^2} \frac{\exp[i\omega_q \sqrt{\varepsilon_q}]}{2\sqrt{\varepsilon_q}}. \quad (13)$$

Using the asymptotic expression of the poles (12) and the first order estimate  $\sqrt{\varepsilon_q} \approx 1 - \Omega^2/(2\omega_q^2)$ , the expression above becomes

$$E_p(\tau) \approx -\frac{\omega_s}{2} \sum_q \frac{e^{-i[q\pi\tau + \Omega^2(\tau+1)/(2q\pi)]}}{(q\pi)^2 (2q\pi/\Omega)^{2\tau}} \left[ 1 + \frac{\Omega^2/2}{q^2\pi^2} \right], \quad (14)$$

where  $\tau = t - t_0$  ( $t - 1$  in normalized units) is the relative time. All the poles corresponding to  $q \in \mathbb{Z}$  are considered, and then the discrete sum can be directly translated to the integral,

$$E_p(\tau) \approx -\frac{\omega_s}{2\pi} \mathcal{P} \int d\omega \frac{e^{-i[\omega\tau + \Omega^2(1+\tau)/(2\omega)]}}{\omega^2 (2\omega/\Omega)^{2\tau}} \left[ 1 + \frac{\Omega^2/2}{\omega^2} \right], \quad (15)$$

where the symbol  $\mathcal{P}$  means that the Cauchy principal value of the integral is considered. It can be checked that, for  $\tau > 0$ , the integral over the semi-circle  $C_R^-$  with radius  $R \rightarrow \infty$  in the lower part of the complex plane of frequencies (with negative imaginary part) vanishes.

Also, it can be shown that the same integral over the semi-circle  $C_\rho^+$  with radius  $\rho$  tending to zero in the upper part of the complex plane of frequencies (with positive imaginary part) tends to zero. Indeed, let  $\omega = \rho \exp[i\phi]$  and consider the integral in Eq. (15) on the path with  $\phi$  varying from  $\sqrt{\rho}$  to  $\pi - \sqrt{\rho}$ . Then, for  $\rho \ll 1$  the integral is bounded by

$$\int_0^\pi d\phi \frac{e^{[\rho\tau - \Omega^2(1+\tau)/(2\sqrt{\rho})]}}{\rho (2\rho/\Omega)^{2\tau}} \left[ 1 + \frac{\Omega^2/2}{\rho^2} \right] \xrightarrow{\rho \rightarrow 0} 0. \quad (16)$$

Hence, adding the vanishing integrals along  $C_\infty^-$  and  $C_0^+$ , the integral expression can be written as

$$E_p(\tau) \approx -\frac{\omega_s}{2\pi} \int_C d\omega \frac{e^{-i[\omega\tau + \Omega^2(1+\tau)/(2\omega)]}}{\omega^2 (2\omega/\Omega)^{2\tau}} \left[ 1 + \frac{\Omega^2/2}{\omega^2} \right], \quad (17)$$

where  $C$  is a closed loop around the origin  $\omega = 0$  and negatively oriented. This loop can be deformed, as soon as the origin remains inside, since the function under the integral in Eq. (15) is analytic in  $\mathbb{C} \setminus \{0\}$ . Thus, taking  $C = U$ , the circle centered at the origin and positively oriented, the following expression of the precursor is obtained,

$$E_p(\tau) \approx \frac{\omega_s}{2\pi} \int_U d\omega \frac{e^{-i[\omega\tau + \Omega^2(1+\tau)/(2\omega)]}}{\omega^2 (2\omega/\Omega)^{2\tau}} \left[ 1 + \frac{\Omega^2/2}{\omega^2} \right]. \quad (18)$$

This integral expression is similar to the one proposed by Sommerfeld in Ref. [2], but with three differences. The first difference is the correction  $\tau$  in the term  $\Omega^2(1+\tau)/(2\omega)$  in the exponential function, which induces a correction in the oscillation period of the Sommerfeld precursor. The second difference is the time-dependent correction factor  $(2\omega/\Omega)^{2\tau}$  decreasing the amplitude of the Sommerfeld precursor. Finally, the third difference is the additional term on the right with the factor  $\Omega^2/(2\omega^2)$  which allows the definition of the precursor after the one of Sommerfeld and before the one of Brillouin. These three corrections lead to significant improvements in the description of the precursor amplitude and periodicity, as shown hereafter.

The expression (18) can be evaluated by choosing the frequencies  $\omega = \nu_\tau e^{i\phi}$  on the circle  $U$  with radius  $\nu_\tau$  defined by

$$\nu_\tau = \Omega \sqrt{\frac{1+\tau}{2\tau}}. \quad (19)$$

The following expression is then obtained

$$E_p(\tau) \approx \frac{2\omega_s}{\Omega} \left[ \frac{\Omega}{2\nu_\tau} \right]^{1+2\tau} \frac{i}{2\pi} \int_0^{2\pi} d\phi e^{i[-(1+2\tau)\phi - 2\nu_\tau\tau \cos \phi]} + \frac{4\omega_s}{\Omega} \left[ \frac{\Omega}{2\nu_\tau} \right]^{3+2\tau} \frac{i}{2\pi} \int_0^{2\pi} d\phi e^{i[-(3+2\tau)\phi - 2\nu_\tau\tau \cos \phi]}. \quad (20)$$

The integrals above are close to the Bessel functions of irrational order  $1+2\tau$  and  $3+2\tau$ . Hence, the final obtained

expression for the precursor is

$$E_p(\tau) \approx \frac{2\omega_s}{\Omega} \left[ \frac{\Omega}{2\nu_\tau} \right]^{1+2\tau} J_{1+2\tau}[2\nu_\tau \tau] - \frac{4\omega_s}{\Omega} \left[ \frac{\Omega}{2\nu_\tau} \right]^{3+2\tau} J_{3+2\tau}[2\nu_\tau \tau]. \quad (21)$$

This expression converges to the one obtained by Sommerfeld [2] when  $\tau \rightarrow 0$ . Figure 5 shows the comparison between the different analytical estimates of the precursors and the numerical temporal response for the given test case in Fig. 4.a). It turns out that the new expression (21) obtained by the present method is significantly more accurate than the original one proposed by Sommerfeld. In particular, in Fig. 5, both the amplitude and oscillating frequency of the signal remain well described by the analytical estimate (21) until the arrival of the Brillouin precursor at  $1 + \tau \approx 2$ . The oscillating frequency, defined by

$$\frac{\partial 2\nu_\tau \tau}{\partial \tau} = \Omega \frac{1 + 2\tau}{\sqrt{2\tau(1 + \tau)}}, \quad (22)$$

tends to infinity when  $\tau \rightarrow 0$  and, for large values of  $\tau$ , decreases to  $\Omega\sqrt{2}$ . This asymptotic value  $\Omega\sqrt{2}$  is different from the expected frequency  $\omega_p$  [see Fig. 4.c)], which can be explained by the absence of the poles in the vicinity of  $\omega_p$  in the starting expression (13).

Finally, the relevance of the group velocity for the precursor is discussed. Starting from the normalized dispersion law  $k^2 \approx \omega^2[1 - \Omega^2/(\omega^2 - \omega_0^2)]$ , with  $kd \rightarrow k$  the normalized wavenumber, the group velocity can be estimated for high frequencies:  $\partial\omega/\partial k \approx [1 - \Omega^2/(2\omega^2)]$ . Assuming that the waves travel at this group velocity, the time needed to propagate along the distance  $d$  is given by

$$(1 + \tau) \frac{\partial\omega}{\partial k} = 1 \iff \omega_g(\tau) = \Omega \sqrt{\frac{1 + \tau}{2\tau}}. \quad (23)$$

Hence, it is found that the frequency  $\omega_g(\tau)$  is precisely the radius  $\nu_\tau$  of the circle  $U$  used in the derivation of the precursor, showing the critical role of this frequency corresponding to the group velocity. Moreover, when  $\tau \rightarrow 0$ , the frequency  $\omega_g(\tau) \sim \Omega/\sqrt{2\tau}$  tends to the oscillation frequency (22). However, for values of time  $\tau > 0$ , the oscillating frequency (22) is different from  $\omega_g(\tau)$ , showing that the velocity of each frequency component appears to be more complex than the group velocity, even in this situation of low dispersion occurring at high frequencies.

## V. CONCLUSION

In conclusion, a novel method has been introduced to analyze the wave propagation in dispersive media. The dispersive medium is considered to be bound, which generates a discrete set of complex resonances and modes.

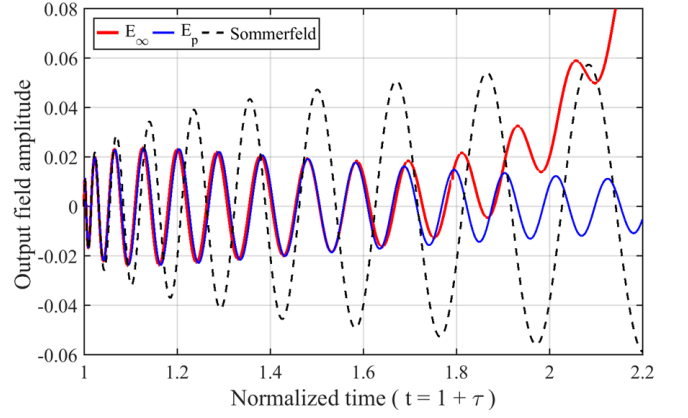


FIG. 5. A comparison between the precursors of a wave propagating in an infinite medium  $E_\infty(t)$  given by (1) (in red), the Sommerfeld precursor original expression [2] (in dashed black), and the precursor  $E_p(\tau)$  given by the novel expression (21) (in blue).

In this case, it is shown that no branch-cut exits in the complex frequency domain. Consequently, a closed-form expression of the transmitted field is derived using the modal expansion. That allows a direct physical interpretation of different components of the transient field as different modes of the system, while these transients are characterized in terms of the oscillation frequency and arrival time. In addition, this method can effectively describe the precursors in infinite dispersive media. A modified analytical expression of the Sommerfeld precursor is derived, which significantly improves the description of the precursor amplitude and oscillation period. In particular, the obtained accuracy for the first oscillations can be exploited to design early detection systems for waves.

The present work shows the relevance of the method using an expansion of the modes of the system and, more generally, the potential of the quasinormal modes expansion [46–48]. The proposed method and results are valid for all waves governed by Helmholtz equations with dispersion subject to causality requirement, e.g. elastic, hydrodynamic, and gravity waves.

## ACKNOWLEDGMENTS

This work was supported by the French National Agency for Research (ANR) under the project “Resonance” (ANR-16-CE24-0013). We would like to express our gratitude to Prof. Aladin Hassan Kamel (Ain-Shams University, Egypt) for the valuable discussions. We acknowledge the anonymous reviewers for their valuable comments.



## Appendix A: Analytic treatment of the poles of the Lorentz medium

In order to evaluate the temporal response of dispersive media, it is required to obtain the set of poles  $\{\omega_q, q \text{ integer}\}$  of the resonator transmission function  $T(\omega)$  in Eq. (4), or in other words, to evaluate all the solutions of  $\omega_q$  for

$$1 - \rho^2(\omega_q) e^{2i\omega_q \sqrt{\varepsilon(\omega_q)}} = 0. \quad (\text{A.1})$$

In this appendix, an asymptotic approach is proposed in order to estimate the poles for the specific case of Lorentz medium with the frequency-dependent permittivity expression:

$$\varepsilon(\omega) = 1 - \frac{\Omega^2}{\omega^2 - \omega_0^2 + i\omega\gamma}. \quad (\text{A.2})$$

This could provide more understanding to the contribution to the temporal response of different types of poles. Notice that the complex frequency domain is symmetric around the imaginary axis, i.e.  $\text{Re}(\omega_{-q}) = -\text{Re}(\omega_q)$ , and  $\text{Im}(\omega_{-q}) = \text{Im}(\omega_q)$ .

The solution is determined in the form  $\omega_q = a(q) - ib(q)$ , where  $a$  and  $b$  are positive real parameters that represent the Free Spectral Range (FSR) and the losses of the resonator at a given frequency, respectively. With these notations, the equation above becomes

$$\rho(\omega_q) = \pm e^{-i\omega_q \sqrt{\varepsilon(\omega_q)}}. \quad (\text{A.3})$$

Assuming lossless media  $\gamma = 0$ , equating the amplitude and the phase parts leads to

$$a(q) = \frac{q\pi}{\sqrt{\varepsilon(\omega_q)}}, \quad (\text{A.4})$$

$$b(q) = -\frac{\ln |\rho(\omega_q)|}{\sqrt{\varepsilon(\omega_q)}}. \quad (\text{A.5})$$

Figure A.1 shows four different zones of the permittivity of a Lorentz medium, where the poles at each zone can be characterized by a distinct feature. Two zones are below resonance  $\omega_0$  and two are above the plasma frequency  $\omega_p = \sqrt{\omega_0^2 + \Omega^2}$ . No poles exist between  $\omega_0$  and  $\omega_p$  where the permittivity is negative and the index is purely imaginary. This leads to a decay of the signal inside the medium, so there is no propagation solution.

The first zone is at low frequencies, where the permittivity is almost constant. The poles in this zone constitute the Brillouin precursor. The second zone is near resonance frequency, where the permittivity is highly dispersive. The third zone is near the plasma frequency,  $\omega_p = 44.7$  in the given example, where  $\varepsilon \approx 0$ . The fourth zone is at high frequencies. The high-frequency poles in both zones 3 and 4 are responsible for the Sommerfeld precursor at the onset of the propagating wave.

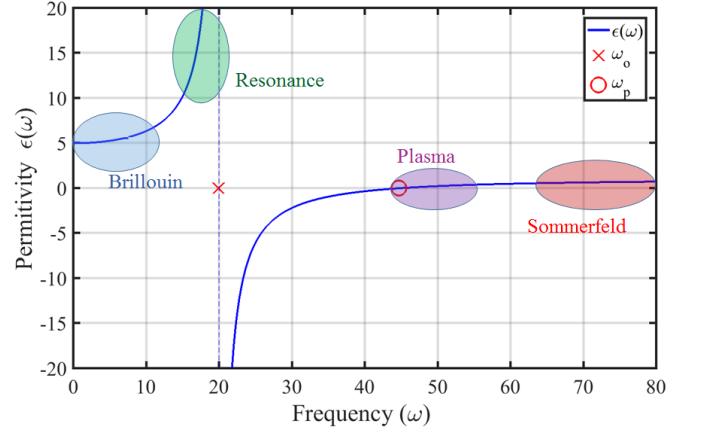


FIG. A.1. The permittivity of a Lorentz medium of  $\omega_0 = 20$ ,  $\Omega = 40$ , and  $\gamma = 0$ . Four distinct zones of poles are indicated.

At each frequency zone in Fig. A.1, a reasonable approximation can be used to formulate a closed-form expression of the poles. The poles between these zones can be determined using an iterative method. Since the amplitude term (reflectivity) is bounded to unity, it is generally correct to assume that  $b(q) \ll a(q)$  and  $|\omega_q| \simeq a$ .

### a. [Zone-1]: Low-frequency (Brillouin precursor)

Starting from  $\omega \ll \omega_0$ , Taylor series can be used at this zone to approximate the permittivity, and the reflectivity in Eq. (3) as

$$\varepsilon(\omega) \underset{\omega \ll \omega_0}{\approx} \varepsilon_s + (\varepsilon_s - 1) \frac{\omega^2}{\omega_0^2}, \quad (\text{A.6})$$

$$\rho(\omega) \approx \rho_s \left[ 1 + \frac{1}{\sqrt{\varepsilon_s}} \frac{\omega^2}{\omega_0^2} \right], \quad (\text{A.7})$$

where  $\varepsilon_s = 1 + \Omega^2/\omega_0^2$  is the static permittivity at  $\omega = 0$ , and  $\rho_s = \rho(\omega = 0)$ . Since the permittivity is nearly constant in this zone, the real part of the poles can be assumed to be

$$a(q) = \frac{q\pi}{\sqrt{\varepsilon_s}}. \quad (\text{A.8})$$

Using  $|\omega_q| \simeq a$ , it is obtained that

$$b(q) = \frac{\ln |1/\rho_{\omega_s}|}{\sqrt{\varepsilon_s}} - \frac{q^2 \pi^2}{\omega_0^2 \varepsilon_s}. \quad (\text{A.9})$$

Consequently, the poles expression for zone 1 is

$$\omega_q = \frac{q\pi}{\sqrt{\varepsilon_s}} - i \frac{\ln |1/\rho_{\omega_s}|}{\sqrt{\varepsilon_s}} + i \frac{q^2 \pi^2}{\omega_0^2 \varepsilon_s}. \quad (\text{A.10})$$

This expression is valid as long as  $q \ll \sqrt{\varepsilon_s} \omega_0$ .

Since the permittivity is weakly dispersive in this zone, it is possible to use the group velocity approximation in order to estimate the arrival time of the Brillouin precursor (in normalized units) as,

$$t_B = \sqrt{\epsilon_s}. \quad (\text{A.11})$$

*b. [Zone-2]: Near-Resonance ( $\epsilon \rightarrow \infty$ )*

In the near resonance zone  $\omega \simeq \omega_0$ , the permittivity can be approached by

$$\epsilon(\omega) \underset{\omega \rightarrow \omega_0}{\approx} \frac{\Omega^2}{2\omega_0} \frac{1}{\omega_0 - \omega}. \quad (\text{A.12})$$

The poles are found using an iterative method. As a first step, let  $\omega_q = \omega_0 - \zeta^2$ , which implies

$$\sqrt{\epsilon(\omega_q)} \simeq \frac{\Omega}{\sqrt{2\omega_0} \sqrt{(\omega_0 - \omega_q)}} \simeq \frac{\Omega}{\sqrt{2\omega_0}} \frac{1}{\zeta}, \quad (\text{A.13})$$

and, assuming  $\zeta^2 \ll \frac{\Omega^2}{2\omega_0}$ , it is obtained that

$$\rho(\omega_q) \simeq -1 + \frac{2}{\sqrt{\epsilon(\omega_q)}} = -1 + 2 \frac{\sqrt{2\omega_0}}{\Omega} \zeta. \quad (\text{A.14})$$

Taking the logarithm of the square of Eq. (A.3) and using that  $\ln(1+x) \approx x$  for  $x \ll 1$  yield

$$-4 \frac{\sqrt{2\omega_0}}{\Omega} \zeta = iq2\pi - i2 \frac{\Omega}{\sqrt{2\omega_0}} \frac{1}{\zeta} (\omega_0 - \zeta^2). \quad (\text{A.15})$$

Since  $\zeta^2 \ll \frac{\Omega^2}{2\omega_0}$ , the left side can be omitted. In order to reach an expression for  $\zeta$  for the first iteration, it is assumed in addition that  $\zeta^2 \ll \omega_0$ , which leads to

$$\zeta = \frac{\Omega \sqrt{\omega_0/2}}{q\pi}. \quad (\text{A.16})$$

Consequently, the poles expression is, after a first iteration,

$$\omega_q = \omega_0 - \frac{\omega_0 \Omega^2}{2\pi^2 q^2}, \quad (\text{A.17})$$

As expected, no pole exists for frequencies higher than the resonance where the refractive index is complex (metallic region).

To obtain the imaginary part of the poles expression, a second iteration is needed: let now  $\omega_q$  be

$$\omega_q = \omega_0 - \frac{\omega_0 \Omega^2}{2\pi^2 q^2} (1 + \zeta^2). \quad (\text{A.18})$$

Here, it is assumed that  $\zeta^2 \ll 1$ . Similarly to the first iteration, we have

$$\epsilon(\omega_q) \simeq \frac{\pi^2 q^2}{\omega_0^2 (1 + \zeta^2)}, \quad (\text{A.19})$$

and

$$\rho(\omega_q) = -1 + \frac{2\omega_0}{q\pi} \left[ 1 + \frac{\zeta^2}{2} \right]. \quad (\text{A.20})$$

Taking again the logarithm of the square of Eq. (A.3), it is obtained that

$$\begin{aligned} -\frac{4\omega_0}{q\pi} \left[ 1 + \frac{\zeta^2}{2} \right] = \\ iq2\pi - i \frac{2\pi q}{\omega_0} \left[ 1 - \frac{\zeta^2}{2} \right] \left[ \omega_0 - \frac{\omega_0 \Omega^2}{2\pi^2 q^2} (1 + \zeta^2) \right]. \end{aligned} \quad (\text{A.21})$$

Since  $q \gg \Omega$  and  $\zeta^2 \ll 1$ , this implies

$$-\frac{4\omega_0}{q\pi} \approx iq\pi\zeta^2 \implies \zeta^2 = i \frac{4\omega_0}{q^2 \pi^2}. \quad (\text{A.22})$$

The expression of poles obtained after the two iterations is then

$$\omega_q = \omega_0 - \frac{\omega_0 \Omega^2}{2q^2 \pi^2} \left[ 1 + i \frac{4\omega_0}{q^2 \pi^2} \right]. \quad (\text{A.23})$$

This expression is limited to  $q \gg (\sqrt{\omega_0}, \Omega)$ .

The poles in this zone show an accumulation behavior, i.e. an infinite number of poles in the zone near the resonance frequency. However, one can show that the summation of the overall contribution of these infinite poles, in Eq. (9), converges. That's due to the fact that by approaching the resonance frequency, the reflectivity of the interfaces goes to unity owing to the very large permittivity mismatch. Therefore, the transmission function of the resonator vanishes near resonance  $T(\omega \rightarrow \omega_0) \rightarrow 0$ . This can be shown by analyzing the term corresponding to the transmission function of the resonator in Eq. (9),

$$\begin{aligned} \frac{\partial T^{-1}}{\partial \omega}(\omega_q) \underset{\omega_q \approx \omega_0}{\approx} -i \left[ \frac{\omega_0}{4} \frac{\partial \epsilon}{\partial \omega}(\omega_q) \right] \cos[\omega_0 \sqrt{\epsilon_q}] - \\ \left[ \epsilon_q + \frac{2\omega_0 + i}{4} \frac{\partial \epsilon}{\partial \omega}(\omega_q) \right] \frac{\sin[\omega_0 \sqrt{\epsilon_q}]}{\sqrt{\epsilon_q}}, \end{aligned} \quad (\text{A.24})$$

The term  $[\partial \epsilon / \partial \omega](\omega_q)$  depends on  $1/(\omega_0 - \omega_q)^2$ , which in turn, depends on  $q^4$ . The limit of Eq. (10), for  $q \rightarrow \infty$ , tends to  $\infty$ . Hence,  $[(\partial T^{-1})/(\partial \omega)]^{-1} \rightarrow 0$ . That means the higher terms of the summation in Eq. (9) have lower contributions. Furthermore, since  $\sum_{q \in \mathbb{Z}} q^{-4}$  converges, the summation in Eq. (9) converges.

Figure A.2 compares the poles below the resonance, for the given example in Fig. A.1, using a numerical technique (Muller's method) and the poles expressions derived earlier in Eqs. (A.10, A.23). Both results show an excellent agreement in zones 1 and 2, while the derived expressions can be used asymptotically to evaluate the poles in between these zones.

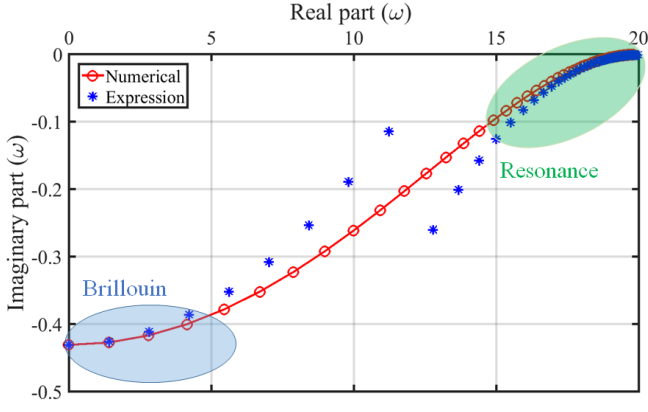


FIG. A.2. The poles below resonance for a Lorentz medium of  $\omega_0 = 20$  and  $\Omega = 40$ . The poles expressions for zone 1 and 2 show excellent agreement with the numerical calculations.

*c. [Zone-3]: Near Plasma frequency ( $\varepsilon \simeq 0$ )*

For the near-plasma zone  $\omega \simeq \omega_p$ , the parameter  $\zeta^2 \ll 1$  is introduced so that,

$$\omega_q = \omega_p(1 + \zeta^2). \quad (\text{A.25})$$

Then the permittivity becomes

$$\varepsilon(\omega) \simeq \frac{2\omega_p^2}{\Omega^2} \zeta^2 \implies \sqrt{\varepsilon(\omega)} \approx \frac{\sqrt{2}\omega_p}{\Omega} \zeta \quad (\text{A.26})$$

and, using that this permittivity is near zero, the reflection coefficient is

$$\rho(\omega) \approx 1 - \frac{2\sqrt{2}\omega_p}{\Omega} \zeta. \quad (\text{A.27})$$

Taking the logarithm of Eq. (A.3) leads to

$$-\frac{2\sqrt{2}\omega_p}{\Omega} \zeta = iq\pi - i\frac{\sqrt{2}\omega_p^2}{\Omega} \zeta(1 + \zeta^2) \quad (\text{A.28})$$

and, using the presumption of  $\zeta^2 \ll 1$ , it is obtained that

$$\zeta = \frac{q\pi\Omega}{\sqrt{2}\omega_p(\omega_p^2 + 4)}(\omega_p - 2i). \quad (\text{A.29})$$

Since the plasma wavelength of materials are mostly in the nanometer region [49], then the slab thickness can be assumed to be much larger than the plasma wavelength. In this situation, the normalized plasma frequency can be safely assumed to be  $\omega_p \gg 1$ . Finally, we reach an expression for the poles near the plasma frequency  $\omega_p$ ,

$$\omega_q = \omega_p \left[ 1 + \frac{q^2\pi^2\Omega^2}{2\omega_p^4} (1 - 4i/\omega_p) \right]. \quad (\text{A.30})$$

The limit of validity for this expression is  $q \ll \frac{\omega_p^2}{\Omega}$  in order to satisfy  $\zeta^2 \ll 1$ .

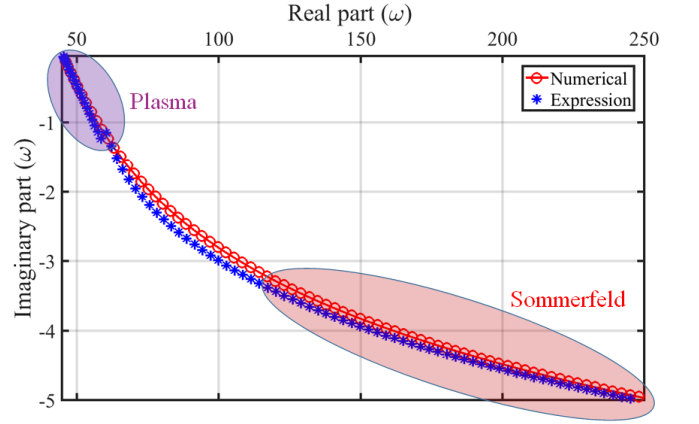


FIG. A.3. The poles above plasma frequency for a Lorentz medium of  $\omega_0 = 20$ ,  $\Omega = 40$  and  $\omega_p = 44.7$ . The poles expressions for zone 3 and 4 are compared with numerical calculations.

*d. [Zone-4] High Frequency (Sommerfeld precursor)*

The medium cannot follow the excitation of the source when  $\omega \gg \omega_0$  and behaves like the vacuum with a group velocity  $v_g \rightarrow c$ . Thus, the contribution of the poles of this zone appears at the onset of the transmitted field from the dispersive media.

The permittivity is close to unity  $\varepsilon \simeq 1$ , which leads to

$$\sqrt{\varepsilon(\omega)} \simeq 1 - \frac{\Omega^2/2}{\omega^2 - \omega_0^2}, \quad (\text{A.31})$$

and then implies

$$\rho(\omega) \simeq \frac{\Omega^2/4}{\omega^2 - \omega_0^2} \simeq 0. \quad (\text{A.32})$$

Hence, from (A.4) and (A.5), it is obtained that

$$a(q) = q\pi, \quad b(q) = \ln \frac{q^2\pi^2 - \omega_0^2}{\Omega^2/4}. \quad (\text{A.33})$$

After a second iteration, the poles expression is

$$\omega_q = q\pi + \frac{\Omega^2/2}{q\pi} - i \ln \frac{q^2\pi^2 - \omega_0^2}{\Omega^2/4}. \quad (\text{A.34})$$

This expression for frequency poles remains valid as soon as  $\pi^2 q^2 \gg \omega_0^2 + \Omega^2/4$ .

Figure A.3 shows the poles above the plasma frequency using both the numerical technique and the expressions derived in Eqs. (A.30, A.34). Both results show an excellent agreement in zones 3 and 4.

## Appendix B: Effect of absorption

The effect of absorption on the poles of a dispersive resonator is briefly discussed. The absorption indicates an energy transfer between the incoming wave and



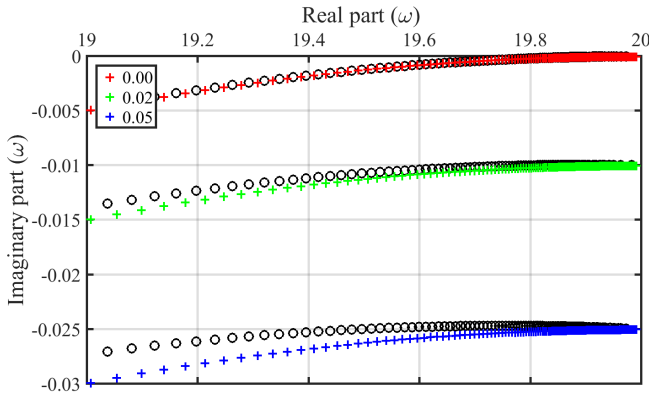


FIG. B.1. The poles near the resonance frequency of a Lorentz medium of  $\omega_0 = 20$  and  $\Omega = 40$  for different values of the absorption coefficients  $\gamma = 0, 0.02$  and  $0.05$ . The poles expressions of zone 2 for the lossy case [+, Eq. (B.1)] is compared with numerical calculations [o].

the medium. Assuming a weakly-absorbing dispersive medium ( $\gamma \ll \omega_0$ ), it can be expected to have a significant absorption in the resonance region. In this case, the expression of poles in zone 2 needs to be modified. The absorption leads to a change in the imaginary part of the poles of the resonator. The modified expression for the poles can be obtained near resonance using the lossy expression of the permittivity provided in Eq. (A.2), by replacing  $\omega_0$  by  $\omega_0 - i\gamma/2$  in the expression of the poles of zone 2: Eq. (A.23). The poles are then given by

$$\omega_q \approx \omega_0 - \frac{\omega_0 \Omega^2}{2q^2 \pi^2} \left[ 1 + i \frac{4\omega_0}{q^2 \pi^2} + i\gamma \frac{q^2 \pi^2}{\omega_0 \Omega^2} \right]. \quad (\text{B.1})$$

In this case, the imaginary part of the poles is affected by both the medium absorption and the reflectivity of the interfaces of the slab. Figure B.1 compares the poles near-resonance obtained by numerical analysis and by the expression of the lossy case given by Eq. (B.1) for different values of the absorption coefficient. Both results are matched in the zone near the resonance.

- 
- [1] A. Sommerfeld, *Ann. Phys.* **349**, 177 (1914).
  - [2] L. Brillouin, *Wave propagation and group velocity*, Vol. 8 (Academic Press, 2013).
  - [3] M. D. Stenner, D. J. Gauthier, and M. A. Neifeld, *Nature* **425**, 695 (2003).
  - [4] K. E. Oughstun and G. C. Sherman, *Phys. Rev. A* **41**, 6090 (1990).
  - [5] N. A. Cartwright and K. E. Oughstun, *SIAM Rev* **49**, 628 (2007).
  - [6] R. Albanese, J. Penn, and R. Medina, *J. Opt. Soc. Am. A* **6**, 1441 (1989).
  - [7] S.-H. Choi and U. Österberg, *Phys. Rev. Lett.* **92**, 193903 (2004).
  - [8] E. Renzi and F. Dias, *J. Fluid Mech* **754**, 250 (2014).
  - [9] P. Pleshko and I. Palócz, *Phys. Rev. Lett.* **22**, 1201 (1969).
  - [10] J. Aaviksoo, J. Kuhl, and K. Ploog, *Phys. Rev. A* **44**, R5353 (1991).
  - [11] M. Sakai, R. Nakahara, J. Kawase, H. Kunugita, K. Ema, M. Nagai, and M. Kuwata-Gonokami, *Phys. Rev. B* **66**, 033302 (2002).
  - [12] H. Jeong, A. M. C. Dawes, and D. J. Gauthier, *Phys. Rev. Lett.* **96**, 143901 (2006).
  - [13] M. J. Frankel and J. L. Birman, *Phys. Rev. A* **15**, 2000 (1977).
  - [14] R. Uitham and B. J. Hoenders, *Opt. Commun* **262**, 211 (2006).
  - [15] E. Varoquaux, G. A. Williams, and O. Avenel, *Phys. Rev. B* **34**, 7617 (1986).
  - [16] E. Falcon, C. Laroche, and S. Fauve, *Phys. Rev. Lett.* **91**, 064502 (2003).
  - [17] V. G. Veselago, *Sov. Phys. Usp.* **10**, 509 (1968).
  - [18] J. B. Pendry, *Phys. Rev. Lett.* **85**, 3966 (2000).
  - [19] M. Notomi, *Phys. Rev. B* **62**, 10696 (2000).
  - [20] B. Gralak, S. Enoch, and G. Tayeb, *J. Opt. Soc. Am. A* **17**, 1012 (2000).
  - [21] J. B. Pendry, D. Schurig, and D. R. Smith, *Science* **312**, 1780 (2006).
  - [22] U. Leonhardt, *Science* **312**, 1777 (2006).
  - [23] D. Schurig, J. J. Mock, B. J. Justice, S. A. Cummer, J. B. Pendry, A. F. Starr, and D. R. Smith, *Science* **314**, 977 (2006).
  - [24] B. Gralak and A. Tip, *J. Math. Phys.* **51**, 052902 (2010).
  - [25] R. E. Collin, *Prog. Electromagn. Res. B* **19**, 233 (2010).
  - [26] W. H. Wee and J. B. Pendry, *Phys. Rev. Lett.* **106**, 165503 (2011).
  - [27] B. Gralak and D. Maystre, *C. R. Physique* **13**, 786 (2012).
  - [28] A. Archambault, M. Besbes, and J.-J. Greffet, *Phys. Rev. Lett.* **109**, 097405 (2012).
  - [29] B. Gralak, G. Arismendi, B. Avril, A. Diatta, and S. Guenneau, *Phys. Rev. B* **93**, 121114(R) (2016).
  - [30] K. E. Oughstun and H. Xiao, *Phys. Rev. Lett.* **78**, 642 (1997).
  - [31] A. V. Alejos, M. Dawood, and F. Falcone, *IEEE Trans. Antennas Propag.* **60**, 5900 (2012).
  - [32] R. A. Handelsman and N. Bleistein, *Arch. Rational Mech. Anal.* **35**, 267 (1969).
  - [33] K. E. Oughstun and G. C. Sherman, *J. Opt. Soc. Am. B* **5**, 817 (1988).
  - [34] K. E. Oughstun and G. C. Sherman, *J. Opt. Soc. Am. A* **6**, 1394 (1989).
  - [35] B. Macke and B. Ségard, *Phys. Rev. A* **86**, 013837 (2012).
  - [36] K. E. Oughstun, *Proc. IEEE* **79**, 1379 (1991).
  - [37] B. Macke and B. Ségard, *Phys. Rev. A* **80**, 011803 (2009).
  - [38] K. E. Oughstun, *Electromagnetic and Optical Pulse Propagation 2: Temporal Pulse Dynamics in Dispersive Attenuative Media*, Vol. 2 (Springer Science & Business Media, 2009).
  - [39] G. Cesini, G. Guattari, G. Lucarini, and C. Palma, *J. Mod. Opt.* **24**, 1217 (1977).
  - [40] C. Kittel, *Introduction to Solid State Physics*, 6th ed. (John Wiley & Sons, Inc., New York, 1986).

- [41] H. van der Lem, A. Tip, and A. Moroz, J. Opt. Soc. Am. B **20**, 1334 (2003).
- [42] J.-M. Combes, B. Gralak, and A. Tip, Contemporary Mathematics *Waves in Periodic and Random Media* **339**, 1 (2003).
- [43] Y. Brûlé, B. Gralak, and G. Demésy, J. Opt. Soc. Am. B **33**, 691 (2016).
- [44] A. Raman and S. Fan, Phys. Rev. Lett. **104**, 087401 (2010).
- [45] D. E. Muller, Math. tables other aids comput. **10**, 208 (1956).
- [46] C. Sauvan, J.-P. Hugonin, I. S. Maksymov, and P. Lalanne, Phys. Rev. Lett. **110**, 237401 (2013).
- [47] Q. Bai, M. Perrin, C. Sauvan, J.-P. Hugonin, and P. Lalanne, Opt. Express **21**, 27371 (2013).
- [48] B. Vial, F. Zolla, A. Nicolet, and M. Commandré, Phys. Rev. A **89**, 023829 (2014).
- [49] M. Dressel and G. Grüner, *Electrodynamics of Solids: Optical Properties of Electrons in Matter*, (Cambridge University Press, 2002).